

EXPERIMENTAL INVESTIGATION ON MICROSTRUCTURE AND MECHANICAL PROPERTIES OF Al-Zn-Mg-Sc ALLOYS

P. K. MANDAL

Department of Metallurgical and Materials Engineering, Indian Institute of Technology Roorkee (IITR), Roorkee, UK, India

ABSTRACT

Microstructures of as-cast Al-Zn-Mg alloys with and without Sc were investigated by optical microscopy, field emission scanning electron microscopy (FESEM) and energy dispersion spectrum analysis. The differential scanning calorimetry (DSC) is employed to identification the phase transformation phenomena through endothermic and exothermic reactions. The effects of Sc on the mechanical properties, recrystallization behavior and age-hardening characteristic of Al-Zn-Mg alloys were studied. The results show that the addition of Sc on Al-Zn-Mg alloy is capable of refining grains obviously. The addition of Sc can improve the strength considerably by strengthening mechanisms of precipitation and grain refinement. With the addition of Sc into Al-Zn-Mg alloy, the ageing process is quickened and the age-hardening effect is heightened. The precipitation of Al_3Sc at different ageing temperatures gave significant additional hardening. The increase the strength and elongation in the alloys is related to the refine grain strengthening, precipitation particles strengthening and substructure strengthening principles.

KEY WORDS: As-cast, Grain Refinement, Ageing, Phase Transformation, Strengthening Mechanisms Etc

Received: Mar 20, 2016; **Accepted:** Mar 30, 2016; **Published:** Apr 09, 2016; **Paper Id.:** IJMPERDAPR20167

INTRODUCTION

The aluminium alloys (7xxx) having the greatest responses to age hardening are based on the Al-Zn-Mg system. Their excellent combination of low density and high strength make them very attractive materials for the transportation and aerospace industry [1-6]. When Al-Zn-Mg is aged to gain its high strength, heterogeneous precipitation occurs on the grain boundaries, making the alloy brittleness [7]. Scandium is sparingly soluble in aluminium in the solid state and supersaturated solid solution decomposes on ageing at elevated temperature, precipitating the Al_3Sc ($L1_2$) phase. Therefore, significant improvement in properties has been found for Sc additions in the range 0.2 to 0.6 wt% in present alloys [8]. In accordance with the heterogeneous nucleation theory [9], the refinement of the grain size of the cast metals is determined by the number of nuclei in melt as well as their nucleating effectiveness depends on the relationship between the lattice types and parameters of the particles and $\alpha(Al)$ matrix, while the similarity in lattice types plays an important role in grain refining. It was reported [10, 11] that eutectic reaction $L \rightarrow \alpha(Al) + Al_3Sc$ at 655 °C exists in Al side of Al-Sc binary system. The eutectic containing 0.55% Sc have a maximum solution in aluminium of 0.35%. With $L1_2$ type fcc lattice ($AuCu_3$ structure) and $a=0.4103$ nm, similar to that of $\alpha(Al)$ ($a=0.4088$), Al_3Sc may serve as heterogeneous nuclei during solidification to refine the grain size in as-cast structure. In general, the elements which have the lower solid solubilities in aluminium have the larger binding energies between the element and vacancies [12]. Therefore, the strengthening effect originates from the formation of fine and highly dispersed Al_3Sc coherent precipitates during ageing that interact with moving dislocations, the formation of a recrystallization-resistant structure and the thermally stable and remain insoluble at high temperatures [13]. It is apparent that, the addition of minor Sc obtains equiaxed structure,

the dendritic structure and the second-phase within the grains disappears completely. In this work, the mechanism of the effect of Sc addition on grain refinement and enhance strength of Al-Zn-Mg alloy is investigated.

EXPERIMENTAL PROCEDURE

The six types of aluminium alloys were prepared by cast metallurgy with pure Zn, pure Mg and masteralloy Al-2%Sc. Basically, prepared alloys were 7xxx series of Al-Zn-Mg without and with Sc addition. The chemical composition was determined by inductively coupled plasma atomic emission spectroscopy (ICP-AES) and atomic absorption spectroscopy (AAS) methods and results are shown in Table 1. The muffle furnace ($\pm 5^\circ\text{C}$) was used to melt the alloys at 780°C . The melt was cast in an air by a steel mould in plate shape ($150 \times 90 \times 8 \text{ mm}^3$). The as-cast alloys were solution treated at $465^\circ\text{C}/1 \text{ h}$ then quenching in water. Then, the experimental alloys were kept in room temperature for seven days for natural ageing. Then, the artificial ageing was performed in tubular furnace ($\pm 2^\circ\text{C}$) at different temperatures at 120°C , 140°C and 180°C respectively. The hardness was measured via Vicker's hardness tester (Model: FIE VM 50) with 10 kgf load at different time intervals 5, 15, 30, 60, 120, 240, 360, 480, 600, 720, 960 and 1200 min. The hardness values were recorded immediately after ageing and continued for 20 h at above interval. The metallographic specimens were examined under optical microscope after etching with a modified Keller's reagent (2.5 ml $\text{HNO}_3 + 1.5 \text{ ml HCl} + 1 \text{ ml HF} + 95 \text{ ml water}$). The as-cast samples were analyzed by electron probe microanalysis (EPMA) with EDS to examine segregation on grain boundary. The ageing kinetics was determined using hardness measurement. The activation energy (E_a) was determined using Arrhenius equation. The second-phase precipitation was revealed by field emission scanning electron microscopy (FESEM) with EDX. Information on the phase transitions through endothermic and exothermic reactions occurring was obtained by differential scanning calorimetry (DSC), using a nitrogen atmosphere and a constant heating rate of $10^\circ\text{C}/\text{min}$. Before, DSC the alloys were solution treated then aged at $140^\circ\text{C}/6 \text{ h}$. Tensile samples were taken from the as-cast plates. Tensile specimens having 5 mm gauge diameter and 25 mm gauge length were tested using Instron tensile testing machine at a tensile speed of 1 mm/min at RT. The as-cast grain size was measured by the mean linear intercept method.

Table 1: Chemical Composition of Studied Alloys (in wt %)

Alloy Nos.	Chemical Composition						Zn+Mg	Zn/Mg Ratio
	Zn	Mg	Sc	Si	Fe	Al		
Alloy-1	6.65	2.9	-	0.03	0.01	Balance	9.55	2.30
Alloy-2	6.95	2.8	-	0.04	0.03	Balance	9.75	2.48
Alloy-3	10.33	3.9	-	0.04	0.02	Balance	14.23	2.65
Alloy-4	6.7	2.8	0.20	0.02	0.04	Balance	9.50	2.39
Alloy-5	6.6	3.81	0.39	0.01	0.02	Balance	10.41	1.73
Alloy-6	5.93	2.9	0.45	0.10	0.19	Balance	8.83	2.04

RESULTS

The as-cast alloys chemical composition are determined by ICP-AES and AAS methods, is shown in Table 1. The optical micrographs of the studied alloys are shown in Figure 1. Coarsened as-cast grains, dendritic structures and severe segregation can easily be observed in the Alloy-1 and Alloy-2 without Sc addition [Figure 1,a-b]. While, the Alloy-3 is

very high Zn+Mg content to eliminate grain boundary segregation and dendritic structure. Therefore, can obtain fine grain structure [Figure 1, c]. On the otherhand, minor Sc can significantly refine the as-cast grain in the Alloy-4 to Alloy-6. In the Alloy-4 minor Sc (0.2%) addition cannot refine dendritic structure but for Alloy-5 and Alloy-6 dendritic structure completely disappeared to obtain fine average grains sizes of 35.7 μm and 28.8 μm respectively [Figure 1,(e-f)]. After solution treatment, the alloys [Figure 2,(a-d)] exhibits obvious equiaxed recrystallized microstructure and homogenization of solute concentration in the matrix. The EPMA spot analysis reveals grain boundary segregation of solute atoms in the as-cast Alloy-2 and Alloy-5 [Figure 3, (a-b)]. Similarly, FESEM with EDS analysis of as-cast Alloy-2 and Alloy-5 exhibits grain boundary segregation of impurity elements [Figure 4, (a-b)]. The artificial ageing has carried out to all six present alloys to following temperatures at 120 $^{\circ}\text{C}$, 140 $^{\circ}\text{C}$ and 180 $^{\circ}\text{C}$ respectively [Figure 5, (a-c)]. The ageing kinetics has been characterized by Vicker's hardness measurement and activation energy. The activation energy (E_a) has been calculated by Arrhenius equation by plotting $\ln(\Delta\text{HV})$ versus $1/T$, the slope of the linear regression fitting is shown in Figure 6(a,b) of Alloy-6 and Alloy-1. The values of activation energies of studied alloys are shown in Table 2. Similarly, the DSC analysis implies precipitation and dissolution of metastable and stable phases in Alloy-1 and Alloy-5 at heating rate 10 $^{\circ}\text{C}/\text{min}$ in nitrogen atmosphere [Figure 7,(a-b)]. The detailed analysis of DSC data indicates that compositional variations of studied alloying elements have significantly effects the on the formation and dissolution of GP zones, η , η' and T phases [in Table 3]. The mechanical properties and grain size of studied as-cast alloys are shown in Table 4.

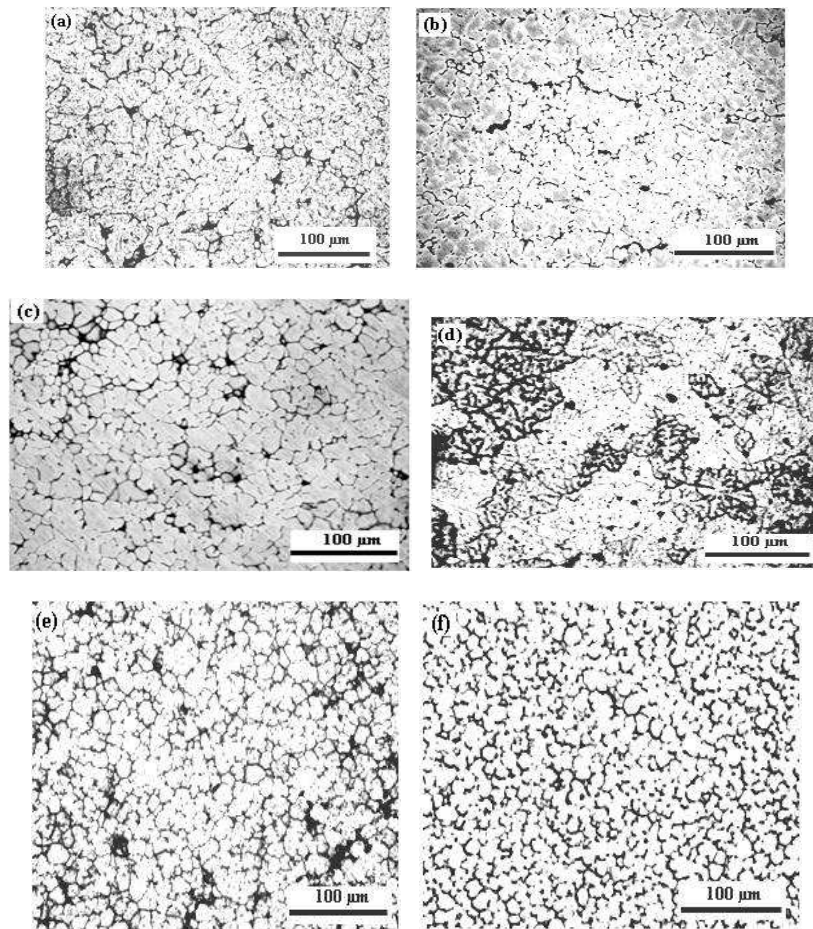


Figure 1: All Optical Micrographs are as-Cast Condition: (a) Alloy-1, (b) Alloy-2, (c) Alloy-3, (d) Alloy-4, (e) Alloy-5, (f) Alloy-6

DISCUSSIONS

In this work, it is important to mention that although the Al-Zn-Mg alloys has been widely studied due to the excellent mechanical properties reached after age hardening, because of the precipitation which occurs through a complex sequence of formation of Guinier-Preston (GP) zones during the decomposition of the supersaturated α -Al solid solution, involving the metastable η' phase and the stable η phase, and as a result of the combination of both low density and high strength have made aluminium alloys the primary materials to be used in the aircraft and automotive industries[14]. Furthermore, age hardening is a function of Zn:Mg ratio to influence both the ageing kinetics and final microstructure. The Zn:Mg ratio control the Zn-bearing constituents. When this ratio over two is formed η (MgZn₂), with lower ratios formed T(Al₂Mg₃Zn₃)[15,16]. If the Zn:Mg ratio is too high, another equilibrium phase, Mg₂Zn₁₁, can also disappear [17]. The grain refining effect of scandium in aluminium alloys is caused equally by two factors: a large number of nuclei in the form of the Al₃Sc particles in a unit of melt volume and high effectiveness of the inoculate action of these particles. Scandium is classified among the 3d transition metals and its reaction with aluminium has particular interest [18]. In general, the elements which have the lower solid solubilities in aluminium have the larger binding energies between the element and vacancies. Especially, since the transition element Sc have quite low solubility only 0.35wt% at eutectic point (0.55 wt% Sc) in Al-Sc phase diagram, then they are considered to have large binding energy. In addition, they also have quite low diffusivity in aluminium. Once the transition elements capture the large amount of vacancies due to their large binding energies, they suppress the free migration of vacancies because they diffuse fairly slowly, that is, the transition elements decrease the number of vacancies which contribute to diffusion in the matrix phase and suppress the diffusion rates in the matrix [19, 12].

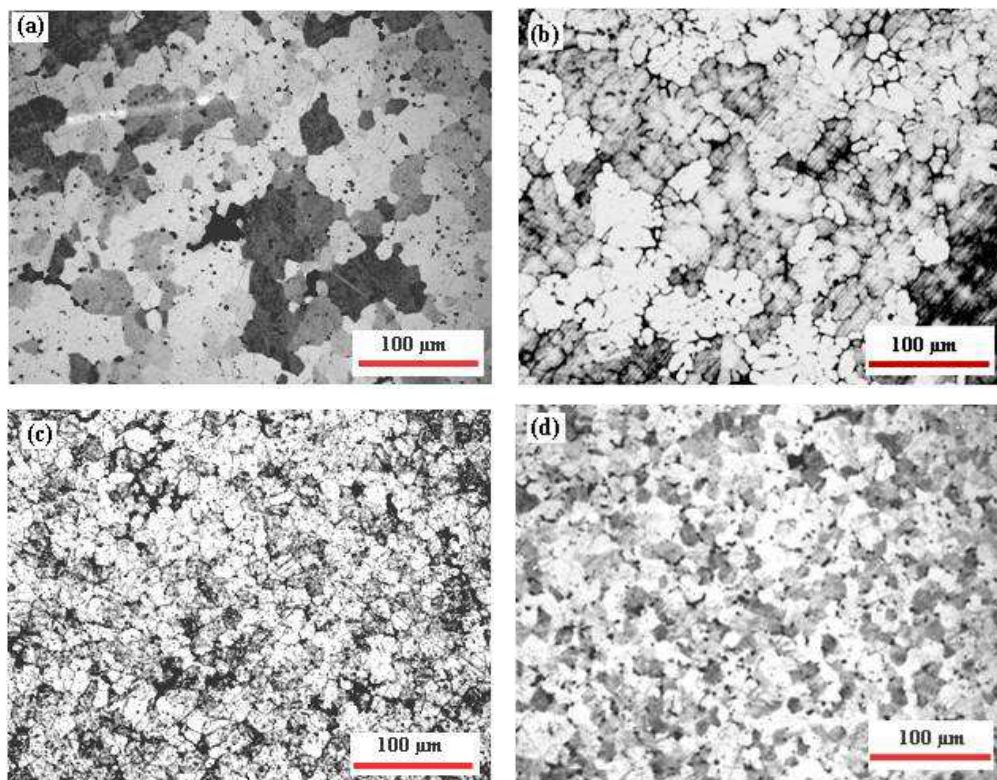


Figure 2: All Optical micrographs are Solution Treated and Water quenched:
(a) Alloy-2, (b) Alloy-3, (c) Alloy-5, (d) Alloy-6

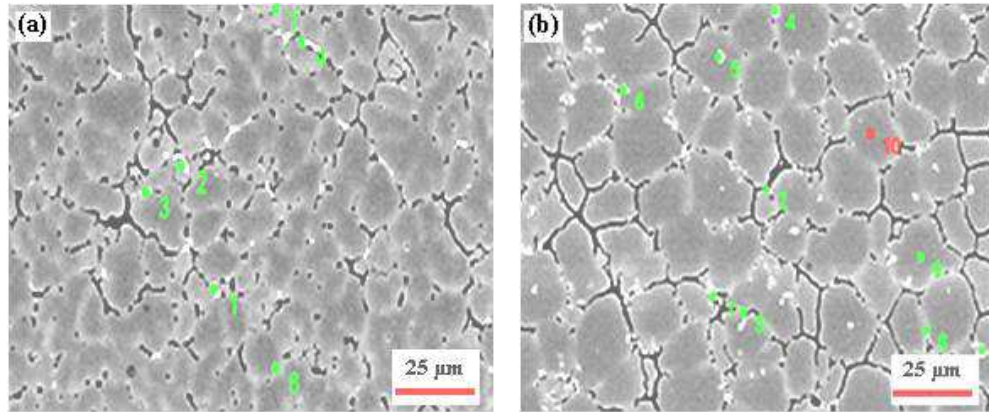


Figure 3: EPMA Spot Analysis of as-Cast Condition: (a) Alloy-2; (b) Alloy-5

The common feature of Al-Zn-Mg alloy is prone to grain boundary segregation of solute elements, which has shown in EPMA spot analysis of as-cast Alloy-2 and Alloy-5 [in Figure 3], respectively. The concentration of elements decrease from grain boundary to grain interior. Therefore, the homogenization treatment is required to eliminate severe dendritic segregation in as-cast alloys. Generally, the relationship between the diffusion coefficient and the temperature can be described as: $D = D_0 \exp\left(\frac{-Q}{RT}\right) \dots (1)$, Where, D_0 is the diffusion coefficient; R is the mole gas constant, Q is the diffusion activation energy; T is thermodynamic temperature [20, 21]. Precipitation of Al_3Sc may take place at the temperature for the solution heat treatment of Al-Zn-Mg alloys. The Al_3Sc particles formed under this condition, normally termed dispersoids, giving a strong contribution to the alloy strength. However, it is frequently found the Al_3Sc dispersoids are very effective in impeding the movement of grain boundary in the materials. This leads to a good recrystallization resistance and the high temperature stability of the Al-Zn-Mg alloys. The effectiveness of the dispersoids will depend on the size, spacing and distribution. The effectiveness of a dispersoid distribution in preventing recrystallization can be qualified by the calculating the average pinning pressure of the dispersoids, according to Zener pinning equation: $Z = k\left(\frac{f\gamma}{r}\right) \dots (2)$, where, f is the volume fraction of dispersoid particles, γ the energy of the boundary that the dispersoids are pinning, r the mean dispersoid radius and k is a scaling factor. At a critical value of the f/r ratio, the Zener pinning will become sufficient to overcome the driving force or boundary migration and recrystallization will be stalled [22, 23]. Thus, the volume fraction f of Al_3Sc precipitates at the t can be calculated from $f = (C_0 - C)/(C_p - C_e)$, where C_p is the Sc concentration in the Al_3Sc phase and C_0 is an initial Sc concentration, C_e is the solid solubility of Sc in the Al matrix and C is the solute concentration in solid solution at time t . Also, precipitate number density N_v of the Al_3Sc precipitates can be calculated from $N_v = 3f/(4\pi r^3)$, r is the average precipitate radius at ageing time t . For each ageing temperature, C rapidly decreases at the initial stage of ageing and, over a time, a linearity is observed between C and $t^{-1/3}$ [24, 25]. The as-cast microstructures are shown in Figure 1(a-f). The dendrites are separated by the coarse phases. The white regions are $\alpha(Al)$ and black regions are eutectic form an almost continuous network with broaden grain boundaries as shown in Sc-free alloys in Figure 1(a-c). Simultaneously, adding of minor Sc can greatly refine the as-cast grain and eliminate dendrites gradually as increased Sc content in Figure 1(d-f).

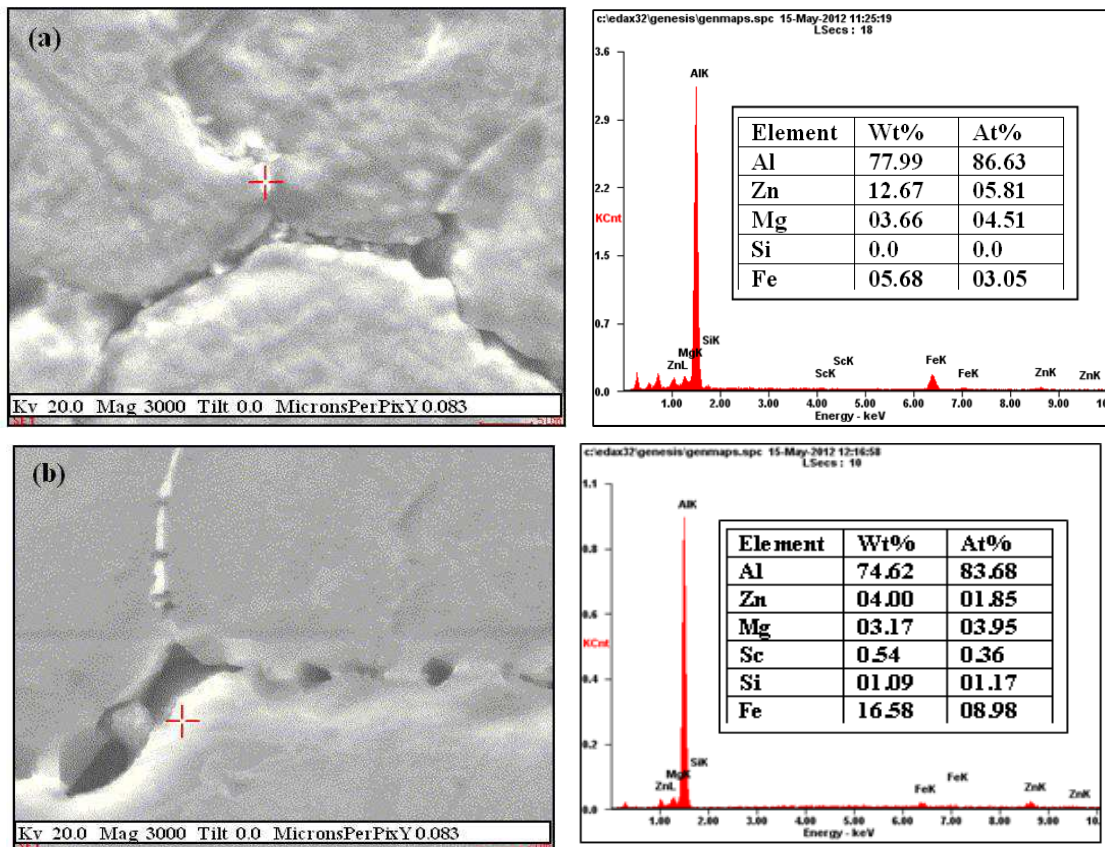


Figure 4: FESEM Micrographs and EDS Analysis of as-Cast Condition: (a) Alloy-2; (b) Alloy-5

During solution treatment [Figure 2, (a-d)] homogenisation occurred, segregation eliminate and alloys become supersaturated solid solution and Al_3Sc particles entered into solid solution and later stages take part as strengthening mechanism or hardening mechanism so far. At this stage, supersaturated solid solution, vacancy creation had occurred which accelerate ageing phenomena of later stages. During strengthening mechanism solute particles, dislocation-vacancy interaction and Al_3Sc particles dispersion wereplayed active role in this stage. In Figure 4(b) FESEM micrograph with EDS analysis shows Sc concentration of Alloy-5. Similarly, EDS analysis of Figure 4(a,b) indicates high percentages of impurity elements Fe and Si, which are detrimental property for ductility and toughness of present alloys. In the Al-Zn-Mg age-hardenable alloys GP zones, η transition phase, $\eta(\text{MgZn}_2)$ and $\text{T}(\text{Al}_2\text{Mg}_3\text{Zn}_3)$ stable phases are forming. However, the structure and composition of the metastable and stable precipitates are strongly dependent on the alloy composition and on the ageing temperature. Further, Sc addition makes it harden due to fine grain and fine dispersion particles which have forming during decomposition of the supersaturated solid solution. An ageing at 120 °C [26], main hardening phase is GP zones and solid solution hardening. In ageing curves, peak hardness achieve within two hours in ageing treatment. But Sc added Alloy-6 shows highest hardening effect in among the ageing curves. Because, due to Sc addition accelerate GP zones formation with Al_3Sc dispersoids impede the recrystallization effect of this Alloy-6. Second highest hardening effect shows Alloy-3, due to high Zn+Mg content to solid solution hardening [Figure 5, (a)].

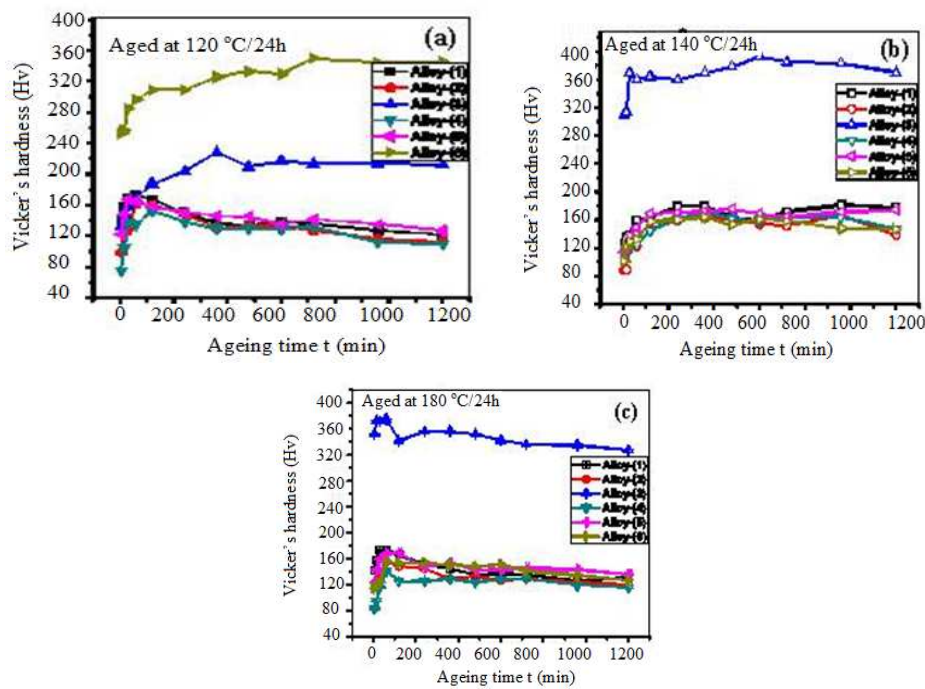


Figure 5: Variation in the Vicker's Hardness with Ageing Time t for the Alloys Aged at: (a) 120 °C; (b) 140 °C and (c) 180 °C

Similarly ageing at 140 °C, only Alloy-3 shows highest hardening effect due to high solute content. Remaining, alloys could not able to show much hardening effect due to overageing stage comes earlier to form stable η phases [Figure 5, (b)]. Similar trend observe an ageing at 180 °C, only Alloy-3 shows highest hardening effect due to high solute content, rest of the alloys fall under overageing stage [Figure 5, (c)]. The activation energy of precipitation can be measured by the following the changes the hardness with temperature and using the Arrhenius relationship, i.e., $\Delta HV = \Delta HV_0 \exp(-E_a/RT)$. By plotting $\ln(\Delta HV)$ vs. $1/T$, the slope of the linear regression fitting will be $-E_a/R$, and the constant ΔHV_0 can be calculated from the intercept with the vertical axis of the linear regression line [Figure 6(a,b)] [27, 28]. The activation particles which have forming during decomposition of the supersaturated solid solution. The activation energy values were in general found to increase with increasing ageing t , time for Sc content Alloy-6. While, the activation energy values were found lower in without Sc content Alloy-1 [Figure 6(b)]. Due to Al_3Sc particles and greater difficulty of migration of dislocations in the presence of dispersoids may higher activation energy achieved for Sc addition Alloy-6 [Figure 6(a)].

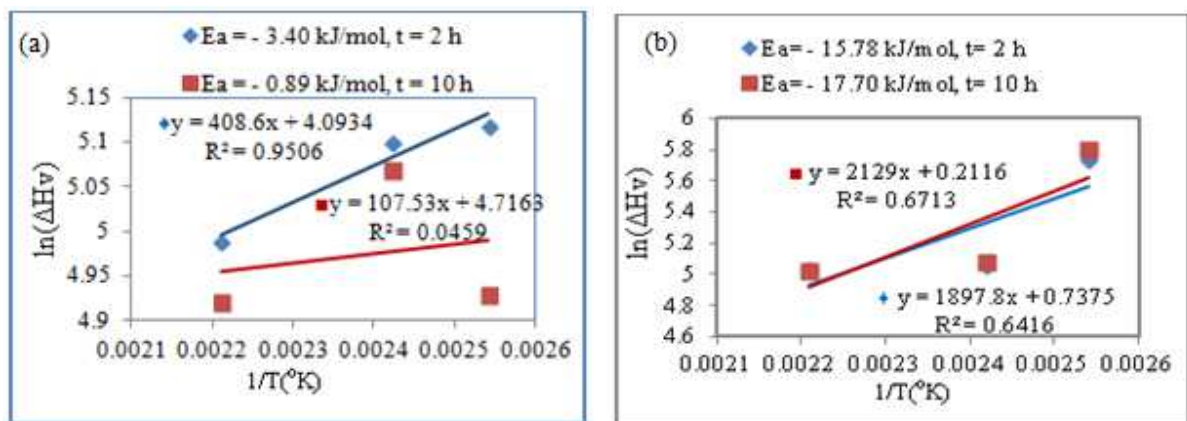


Figure 6: Activation Energy Graphs of: (a) Alloy-1, (b) Alloy-6

Table 2: Activation Energy E_a (kJ/mol) Values Obtained from plots of $\ln(\Delta H_V)$ vs $1/T$

Alloy Nos.	Ageing Time t (Hours)				
	2	6	10	16	20
Alloy-1	- 3.40	- 0.63	- 0.89	-1.83	- 0.67
Alloy-6	- 15.78	- 17.34	- 17.70	- 21.45	- 22.98

Precipitation kinetics in present alloys has been studied by DSC analysis. There two alloys are DSC examined, for Alloy-1(no Sc content) and Alloy-5 (with Sc content) both the curves shows six numbers of endothermic and endothermic peaks throughout the run at 10 °C per min in nitrogen atmosphere. The phase transformations of present 7xxx series alloys mainly involve the formation and dissolution of GP zones, η , η' , T and Al_3Sc phases. The balance properties of 7xxx alloys can be optimized by microstructural modification via alloy compositional changes and heat treatment [29]. Since, both the alloys are aged at 140 °C for 6 h to formation of η' precipitates to precursors of GP zones and η and T phases. For Alloy-1 [Figure 7(a)] in DSC curve at point A (5.6 μW , at 206 °C) formation of η phase because as age-hardening phenomena is formed at 150 to 220 °C range. This is very stable phase and incoherent with the matrix. At point B (4.73 μW , at 257 °C) and C (3.6 μW , at 416 °C) as trend indicates dissolution of η phase as temperatures increases. Similarly, point D indicates T phase formation and point E indicates T phase dissolution and peak F shows again formation of T phase at around 580 °C at 3.8 μW .

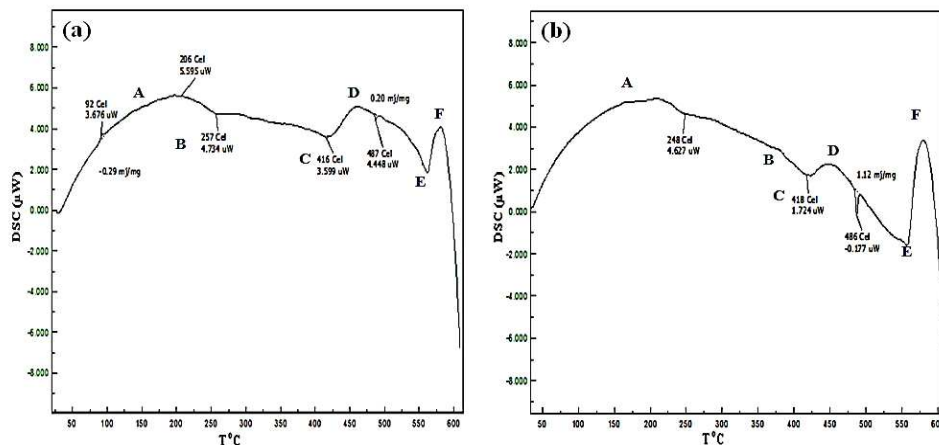


Figure 7: DSC Curves (Solutionized and Aged at 140 °C/6 h) at Heating Rate 10 °C/min: (a) Alloy-1, (b) Alloy-5

For Alloy-5 [Figure 7(b)] contents Sc to shows anti-recrystallization effect with Al_3Sc dispersoids at higher temperature treatment, as shown in DSC run. Similar trend can observe as like Alloy-1 and point F shows larger peak at around 590 °C at 3.85 μW for Alloy-5 [Table 3]. The tensile properties and as-cast grain size are shown in Table 4.

Table 3: Identification of the Main Effects in DSC Curves of Alloy-1 and Alloy-5

Effects→	A	B	C	D	E	F
Alloy-1	η formation η dissolution	η dissolution	η dissolution	T formation	T dissolution	T formation
Alloy-5	η , Al_3Sc formation η dissolution	η dissolution	T, Al_3Sc formation	T dissolution	T dissolution	T, Al_3Sc formation

Table 4: Results of Tensile Properties and Grain Size Measurement in as-Cast Condition

Alloy nos.	As-Cast Condition			
	Grain Size (μm)	$\sigma_{0.2}$ (MPa)	σ_u (MPa)	δ_4 (%)
Alloy-1	35.2	50.5	180.7	2.33
Alloy-2	36.5	52.5	196.9	2.97
Alloy-3	31.3	49.0	166.2	2.52
Alloy-4	30.1	42.5	225.6	3.80
Alloy-5	35.7	58.8	245.7	3.78
Alloy-6	28.8	40.0	302.1	7.10

N.B: yield strength denoted at 0.2% offset from stress-strain curve.

The 0.2% proof stress also marginally increased to indicate good ductile nature of present alloys. The tensile strength and ductility of the Sc content alloys are higher than the without Sc content alloys. The increased Sc level has led to improved ultimate tensile strength and ductility by reducing the volume fraction of the eutectic phases, as well as by fining the grain size [30, 6]. The strengthening mechanism is considered as fine grain strengthening, substructure strengthening and dispersion strengthening by Al_3Sc [31, 2].

CONCLUSIONS

- In the as-cast state the hardness of the supersaturated solid solutions increases with increasing Zn and Mg content due to the solid-solution hardening. Moreover, age-hardening is a function of Zn:Mg ratio to influence both the ageing kinetics and final microstructure. When this ratio over two is formed $\eta(\text{MgZn}_2)$, with lower ratios formed $\text{T}(\text{Al}_2\text{Mg}_3\text{Zn}_3)$.
- In ageing curves, peak ageing achieved within two hours. As ageing progresses, the distance between precipitates is more increased, dislocations bowing are become easier and the hardness is more decreased.
- Thus, minor Sc addition can make the peak ageing arriving earlier for Al-Zn-Mg alloys. Secondary Al_3Sc particles strongly pin sub-boundaries and retard emergence and growth of subgrains, namely substructure strengthening.
- The addition of Sc can retard the recrystallization of the Al-Zn-Mg alloys, increase the recrystallization temperature and significantly refine the recrystallization grains. The reason is the fine Al_3Sc particles anchor the dislocations and the subgrain boundaries, hinder the recombination of the dislocations and the motion of the subgrain boundaries, and so delay the nucleation and growth of the subgrains.
- The presence of Sc resulted in an accelerated formation and growth of η particles, which led to a more rapid increase in the hardness at early stage of ageing at 120 °C.

- The maximum activation energy (E_a) has been found out of 22.98 kJ/mol for Al-Zn-Mg-Sc alloy at 20 h ageing time.
- The DSC analysis has been carried out to identification of the precipitation and dissolution of metastable and stable phases of aluminum alloys.
- The ultimate tensile strength of Al-Zn-Mg-Sc alloys increased gradually as increase Sc content in as-cast condition due to the effect fine dispersion of Al_3Sc precipitates, sub-grain and fine-grain strengthening.

ACKNOWLEDGEMENTS

Author is very much grateful to Council of Scientific & Industrial Research (CSIR), New Delhi for providing financial assistance to carried out this research work in MMED in Indian Institute of Technology Roorkee (IITR), Roorkee.

REFERENCES

1. Ferragut, R., Somoza, A., Dupasquier, A., "On the two-step ageing of a commercial Al-Zn-Mg alloy; a study by positron lifetime spectroscopy," *J. Phys.: Condens. Matter* 8 (1996) 8945-8952.
2. Liang, Z., Qing-lin, P., Yun-bin, H., Chang-zhen, W., Wen-jie, L., "Effect of minor Sc and Zr addition on microstructures and mechanical properties of Al-Zn-Mg-Cu alloys," *Trans. Nonferrous Met. Soc. China* 17(2007)340-345.
3. Jing-zhi, D., Yu-feng, H., Jun, C., "Effect of minor Sc and Zr on microstructures and mechanical properties of as-cast Al-Mg-Si-Mn alloys," *Trans. Nonferrous Met. Soc. China* 19(2009) 540-544.
4. Zhenbo, H., Zhimin, Y., Sen, L., Ying, D., Baochuan, S., Xiang, Z., "Preparation, microstructure and properties of Al-Zn-Mg-Sc alloy tubes," *Journal of Rare Earths*, Vol. 28, No. 4, Aug. 2010, p.641-646.
5. Wenbin, L., Qinglin, P., Liang, Z., Wenjie, L., Yunbin, H. and Junsheng, L., "Effects of minor Sc on the microstructure and mechanical properties of Al-Zn-Mg-Cu-Zr based alloys," *Rare Metals*, Vol. 28, No. 1, Feb. 2009, P. 102-106.
6. Yong-dong, H., Xin-ming, Z., Jiang-hai, Y., "Effect of minor Sc and Zr on microstructure and mechanical properties of Al-Zn-Mg-Cu alloy," *Trans. Nonferrous Met. Soc. China* 16(2006) 1228-1235.
7. Vanderwalker, D. M., Vander Sande, J.B., "Precipitation on low-angle grain boundaries in Al-Zn-Mg," *Metallurgical Transactions A*, Vol. 12A, Oct. 1981, 1787-1414.
8. Parker, B.A., Zhou, Z.F., Nolle, P., "The effect of small additions of scandium on the properties of aluminium alloy," *Journal of Materials Science* 30 (1995) 452-458.
9. Ramachandran, T.R., Sharma, P.K., Balasubramanian, K., "Grain refinement of light alloys", 68th WFC- World Foundry Congress, 7th - 8th February, 2008, pp. 189-193.
10. Zakharov, V.V., "Effect of scandium on the structure and properties of aluminium alloys," *Metal Science and Heat Treatment*, Vol. 45, Nos. 7-8, 2003, pp.246-253.
11. Hyde, K.B., Norman, A.F. and Prangnell, P.B., "The effect of cooling rate on the morphology of primary Al_3Sc intermetallic particles in Al-Sc alloys," *Acta mater.* 49 (2001) 1327-1337.
12. Hisayuki, K., Yamane, T., Takahashi, T., Minamino, Y., Hirao, K., Araki, H., "Diffusion of zinc in commercial Al-Zn-Mg alloys under high pressure," *Journal of Materials Science* 34 (1999) 2449-2454.
13. Tsivoulas, D., Robson, J.D., "Coherency loss of Al_3Sc precipitates during ageing of dilute Al-Sc alloy," *Materials Science Forum*, Vols. 519-521 (2006) pp 473-478.

14. Soto , J., Aramburo , G., Gonzalez,C., Genesca , J., Herrera , R., Juarez-Islas , J.A., "Distribution and prediction of solute in Al-Zn-Mg alloys," *Materials Science &Engineering A* 408(2005) 303-308.
15. Löffler , H., Kovacs , I., Lendvai , J., "Review decomposition processes in Al-Zn-Mg alloys," *Journal of Materials Science* 18 (1983) 2215-2240.
16. Mondolfo , L.F., *Aluminium alloys: structure and properties*, Butterworth, London, 1976.
17. Wolverson , C., "Crystal structure and stability of complex precipitate phases in Al-Cu-Mg-(Si) and Al-Zn-Mg alloys", *Acta. Mater.* 49 (2001) 3129-3142.
18. Davydov,V.G., Rostova,T.D.,Zakharov ,V.V., Filatov ,Y.A., Yelagin ,V.I., " Scientific principles of making an alloying of scandium to aluminium alloys," *Materials Science &Engineering A* 280(2000) 30-36.
19. Chen,Z., Zheng,Z., "Microstructural evolution and ageing behaviour of the low Cu:Mg ratio Al-Cu-Mg alloys containing scandium and lithium", *Scripta Materialia*, 50 (2004) 1067-1071.
20. Yan-hui,H., Yan-xia, Zhi-yi,G., L., Yun-tao,L., Xu,C., "Modeling of whole process of ageing precipitation and strengthening in Al-Cu-Mg-Ag alloys with high Cu-to-Mg mass ratio," *Trans. of Nonferrous Met. Soc. China* 20(2010) 863-869.
21. Du,Y., Chang,Y.A., Huang,B., Gong,W., Jin,Z., Xu,H., Yuan , Z., Liu,Y., He,Y., Xie,F.-Y., "Diffusion coefficients of some solutes in fcc and liquid Al: critical evaluation and correlation," *Materials Science & Engineering A*363 (2003) 140-151.
22. Royset,J., Ryum,N., "Scandium in aluminium alloys," *International Materials Reviews*, 2005, Vol.50, No.1, 19-44.
23. Riddle,Y.W., Sanders, Jr.,T.H., "A study of coarsening, recrystallization, and morphology of macrostructure in Al-Sc-(Zr)-(Mg) alloys," *Metallurgical and Materials Transactions A*, Vol. 35A, January 2004, 341-350.
24. Watanabe,C., Watanabe,D., Monzen,R., "Coarsening behavior of Al₃Sc precipitates in an Al-Mg-Sc alloy," *Materials Transactions*, Vol. 47, No. 9(2006) pp. 2285- 2291.
25. Du,Z.W., Sun,Z.M., Shao,B.L., Zhou,T.T., Chen,C.Q., "Quantitative evaluation of precipitates in an Al-Zn-Mg-Cu alloy after isothermal aging," *Materials Characterization*, 56 (2006) 121-128.
26. Park,J.K., Ardell,A.J., "Microstructures of the commercial 7075 Al alloy in the T651and T7 tempers," *Metallurgical Transactions A*, Vol. 14A, Oct. 1983, 1957-1965.
27. Sha,W., "Activation energy for precipitation hardening and softening in aluminium alloys calculated using hardness and resistivity data," *Physica Status Solidi(a)* 203, No. 8, 1927-1933 (2006).
28. Sha,W., "Application of simple practical models for early stage ageing precipitation kinetics and hardening in aluminium and magnesium composites," *Materials and Design* 28 (2007) 1524-1530.
29. Li , X.M., Starink,M.J., "DSC study on phase transactions and their correlation with properties of overaged Al-Zn-Mg-Cu alloys," *Journal of Materials Engineering and Performance*, Vol. 21(6) June 2012, pp. 977-984.
30. Dai,X-y, Xia,C-q, Wu,A-r, Peng,X-m, "Influence of scandium on microstructures and mechanical properties of Al-Zn-Mg-Cu-Zr alloys", *Materials Science Forum*, Vols. 546-549 (2007) pp. 961-964.
31. Berezina,A.L., Chuistov,K.V., Kolobnev,N.I., Khokhlatova,L.B., Monastyrskaya,T.A., "Sc in aluminium alloys", *Materials Science Forum*, Vols. 396-402, pp. 741-746.

